Jestr

Journal of Engineering Science and Technology Review 6 (4) (2013) 104-114
Special Issue on Recent Advances in Nonlinear Circuits: Theory and Applications

JOURNAL OF
Engineering Science and Technology Review

www.jestr.org

Research Article

Complex Dynamics of FitzHugh-Nagumo Type Neurons Coupled with Gap Junction under External Voltage Stimulation

I. M. Kyprianidis*, and A. T. Makri

Departmentt. of Physics, Aristotle University of Thessaloniki, GR - 54124, GREECE

Received 2 July 2013; Revised 4 September 2013; Accepted 25 September 2013

Abstract

In the present paper, we have studied the complex dynamics of a system of two nonlinear neuronal cells, coupled by a gap junction, which is modelled as a linear variable resistor. The two coupled cells are oscillators of the FitzHugh-Nagumo type. The first cell, the "ImK-cell" is a voltage driven cell, while the second, the "RaLa-cell" is a current driven cell. We have examined the dynamics of the coupled system in the case of bidirectional coupling. An independent voltage source gives the external stimulation. We have examined three different cases (AC, DC, AC plus DC) of the external signal. In each case we have different dynamics. Action potentials, chaotic and periodic oscillations are observed.

Keywords: Nonlinear oscillators, FitzHugh-Nagumo, neuronal cells, gap junction, action potential, chaos, bidirectional coupling.

1. Introduction

Electric circuits with a nonlinear resistor, which is characterized by a smooth cubic υ-i characteristic, have emerged as a simple, yet powerful experimental and analytical tool in studying chaotic behavior in nonlinear dynamics. Among the electrical oscillators that have been studied, the FitzHugh – Nagumo type oscillator [1, 2] is very important, because can simulate neuron cells. The system of two FitzHugh-Nagumo cells coupled with gap junctions, specialized intercellural pathways between adjoining cells, [3], is the simplest possible system simulating two coupled neuron cells via an electric synapse [4]. As introduced by Fitzhugh [1], his model for a spiking neuron is a two dimensional reduction of the Hodgkin – Huxley equations [5]. A qualitative description of the single neuron activity is given, according to FitzHugh, by the system of coupled nonlinear differential equations.

$$\begin{cases} \dfrac{dx}{d\tau} = \gamma\left(x - \dfrac{1}{3}x^3 + y + z \right) \\ \dfrac{dy}{d\tau} = -\dfrac{1}{\gamma}\left(x - \alpha + \beta y \right) \end{cases} \tag{1}$$

The variable x describes the potential difference across the neural membrane and y can be considered as a combination of the different ion channel conductivities, present in the Hodgkin-Huxley model. The control parameter z of the FitzHugh system describes the intensity of the stimulating current. Nagumo et al. [2] proposed an electronic simulator of the model of FitzHugh using a tunnel diode as the nonlinear element.

The FitzHugh model of nonlinear differential equations (1) can be simulated by a different nonlinear electric circuit, [6], using a nonlinear resistor, (Fig.1), with a smooth cubic i–v characteristic given by the following equation (2).

$$i_N = g(\upsilon) = -\frac{1}{\rho}\left(\upsilon - \frac{1}{3}\frac{\upsilon^3}{V_0^2} \right) \tag{2}$$

where ρ and V_0 are normalization parameters. By introducing new, normalized variables

$$\tau = \frac{t}{\sqrt{LC}},\ x = \frac{\upsilon}{V_0},\ y = \frac{\rho i_L}{V_0},\ z = \frac{\rho i_S}{V_0},$$

and applying Kirchhoff's laws we get the state equations (1), where

$$\alpha = \frac{E}{V_0}\ ,\ \beta = \frac{R}{\rho}\ \text{ and }\ \gamma = \frac{1}{\rho}\sqrt{\frac{L}{C}}.$$

* E-mail address: imkypr@auth.gr

ISSN: 1791-2377

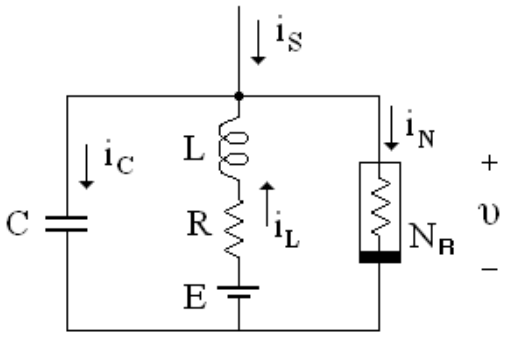

Fig. 1. The electronic simulator of the model of FitzHugh, proposed by Kyprianidis et al [6].

Rajasekar and Lakshmanan proposed a slightly different form of FitzHugh model [7,8] given by the following state equations, which are of Bonhoeffer – van der Pol type,

$$\begin{cases} \dfrac{dx}{d\tau} = x - \dfrac{1}{3}x^3 - y + z \\ \dfrac{dy}{d\tau} = c\left(x + a - by\right) \end{cases} \tag{3}$$

The study of Eqs.(3) revealed the existence of chaotic behavior, following the period doubling route to chaos, and devil's staircases. The nonlinear differential equations (3) can be also simulated by a nonlinear electric circuit, using a nonlinear resistor with a smooth cubic i–v characteristic. The nonlinear electric circuit is shown in Fig.3. The smooth cubic i–v characteristic of the nonlinear resistor of the circuit of Fig.3 is given by the same equation (2), as before.

By introducing new, normalized variables,

$\tau = \dfrac{t}{\rho C}$, $x = \dfrac{\upsilon}{V_0}$, $y = \dfrac{\rho i_L}{V_0}$, and $z = \dfrac{\rho i_S}{V_0}$,

and applying Kirchhoff's laws we get state equations (3), where $a = \dfrac{E}{V_0}$, $b = \dfrac{R}{\rho}$, and $c = \dfrac{\rho^2 C}{L}$.

In the general case, the driving current source has the following form $i_S = I_{DC} + I_0 \cos 2\pi f_S t$ including a DC plus a sinusoidal term of frequency f_S, so

$z = B_{DC} + B_0 \cos 2\pi f t$,

where the normalized frequency f will be $f = \rho C f_S$.

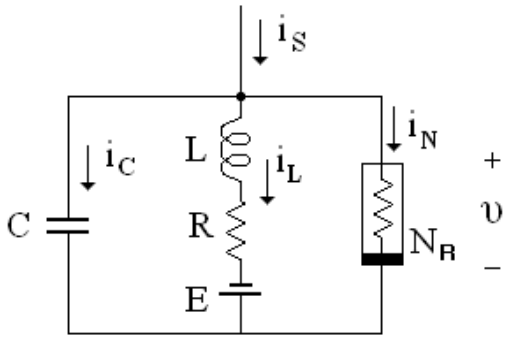

Fig. 2. The nonlinear electric circuit simulating Eqs.(3).

The topology of the circuits of Fig.1 and Fig.2 is exactly the same, proving the equivalence of equations (1) and (3). The circuit of Fig.2 is a current-driven neuron-cell and we call it "RaLa-cell".

2. The FitzHugh – Nagumo Type Circuit Driven by a Voltage Source

In the circuits of Figs.1 and 2, the driving source is a current source. But in most cases, circuits are driven by voltage sources. In this section, we will study the circuit of Fig.2 driven by a voltage source, as it is shown in Fig.3

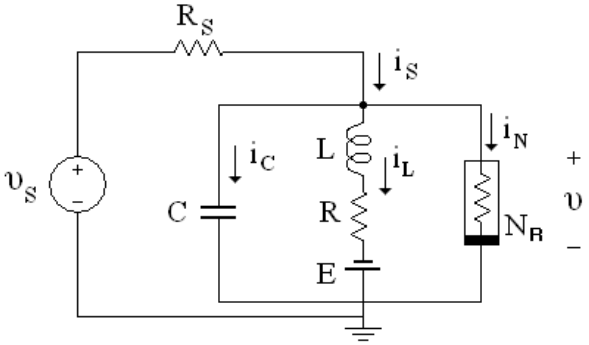

Fig. 3. The circuit of Fig.2 driven by a voltage source.

The smooth cubic i–v characteristic of the nonlinear resistor of the circuit of Fig.3 remains the same as before. By introducing the normalized time $\tau = \dfrac{t}{\rho C}$ and the normalized variables $x = \dfrac{\upsilon}{V_0}$, $y = \dfrac{\rho i_L}{V_0}$, $u = \dfrac{\rho \upsilon_S}{R_S V_0}$ and applying Kirhhoff's laws, we get the following normalized state equations

$$\begin{cases} \dfrac{dx}{d\tau} = x\left(1 - \varepsilon\right) - \dfrac{1}{3}x^3 - y + u \\ \dfrac{dy}{d\tau} = c\left(x + a - by\right) \end{cases} \tag{4}$$

where $a = \dfrac{E}{V_0}$, $b = \dfrac{R}{\rho}$, $c = \dfrac{\rho^2 C}{L}$, and $\varepsilon = \dfrac{\rho}{R_S}$.

In the general case, the driving voltage source has the following form

$$\upsilon_S = V_{DC} + V_m \cos 2\pi f_S t \tag{5}$$

including a DC plus a sinusoidal term of frequency f_S, so

$$u = U_{DC} + U_0 \cos 2\pi f \tau \tag{6}$$

where the normalized frequency f will be $f = \rho C f_S$, while

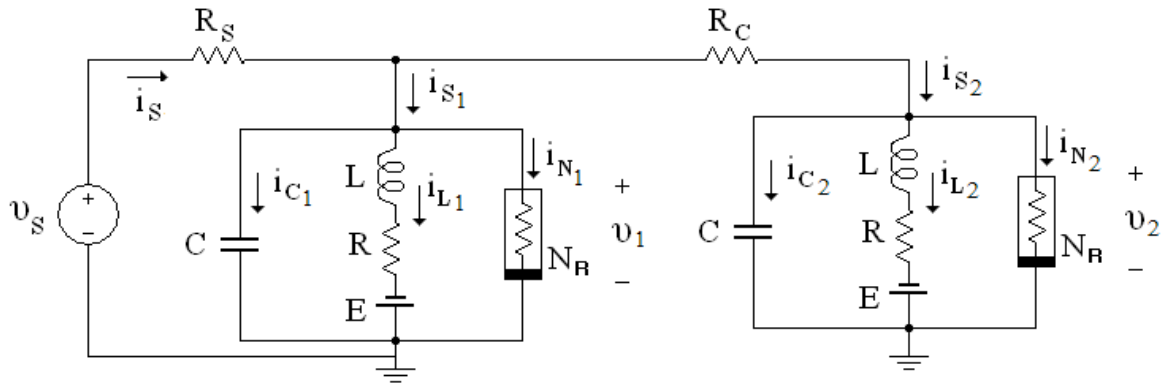

Fig.4. An "ImK-cell" and a "RaLa-cell" coupled via a gap junction (R_C).

$$U_{DC} = \frac{\rho V_{DC}}{R_S V_0} \text{ and } U_0 = \frac{\rho V_m}{R_S V_0}. \quad (7)$$

The circuit of Fig.3 is a voltage driven neuron-cell and we call it "ImK-cell".

3. The Coupled System

By coupling the circuits of Figures 2 and 3 via a linear resistor R_C, we get the system of Fig.4. The two sub-circuits have identical circuit elements, L, R, C, E and N_R. The linear resistor R_C simulates the gap junction between the two neuron–cells [3, 4].

By introducing the normalized time $\tau = \frac{t}{\rho C}$ and the normalized variables

$$x_j = \frac{\upsilon_j}{V_0},\ y_j = \frac{\rho i_{Lj}}{V_0},\ j = 1,2,\ u = \frac{\rho \upsilon_S}{R_S V_0}$$

and applying Kirhhoff's laws, we get the following normalized state equations for the system of Fig. 4.

$$\begin{cases} \dfrac{dx_1}{dt} = x_1(1-\varepsilon) - \dfrac{1}{3}x_1^3 - y_1 - \xi(x_1 - x_2) + u \\ \dfrac{dy_2}{dt} = c(x_1 + a - by_1) \\ \dfrac{dx_2}{dt} = x_2 - \dfrac{1}{3}x_2^3 - y_2 + \xi(x_1 - x_2) \\ \dfrac{dy_2}{dt} = c(x_2 + a - by_2) \end{cases} \quad (8)$$

where $\xi = \frac{\rho}{R_C}$ is the coupling factor, while

$$a = \frac{E}{V_0},\ b = \frac{R}{\rho},\ c = \frac{\rho^2 C}{L}$$

and u is given by Eqs.(6) and (7).

3.1. The system is driven by an AC voltage source

In this case, the constant values of the parameters of the system are a = 0.7, b = 0.8, c = 0.1, ε = 0.150, f = 0.16, and U_{DC} = 0.0. The bifurcation diagram of the complex dynamics of the "ImK-cell", as the normalized amplitude of the voltage source is varied, is shown in Fig. 5.

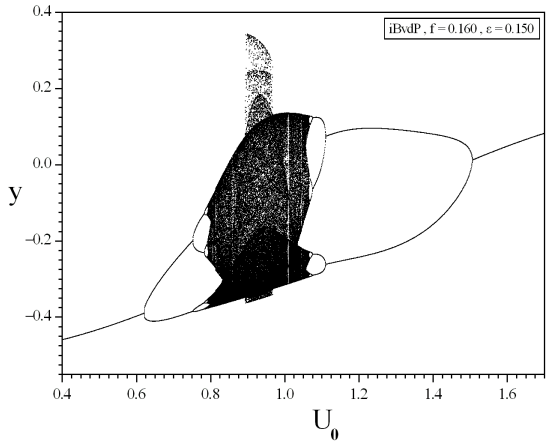

Fig. 5. The bifurcation diagram of the "ImK-cell" as the normalized amplitude of the voltage source is varied. It is a chaotic bubble.

Choosing U_0 = 0.9, corresponding to a chaotic state, the simulation results of state equations (8) give the following bifurcation diagrams versus the coupling factor ξ.

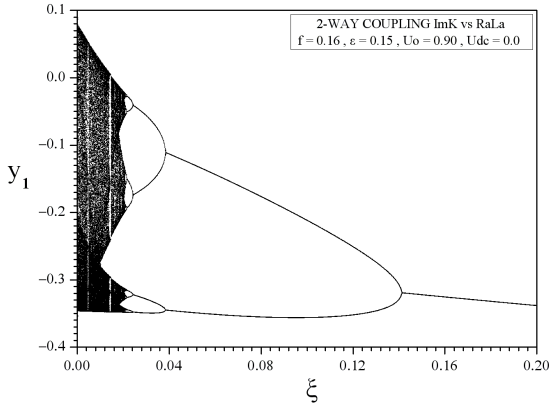

Fig. 6. Bifurcation diagram, y_1 vs. ξ, of the coupling system, under an AC stimulation with U_0 = 0.9.

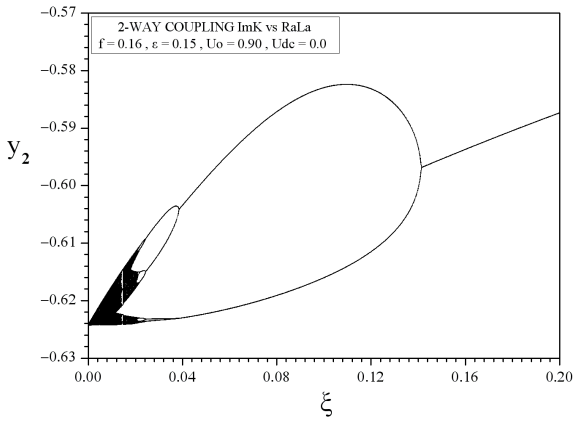

Fig. 7. Bifurcation diagram, y_2 vs. ξ, of the coupling system, under an AC stimulation with $U_0 = 0.9$.

Starting from a chaotic state, the system undergoes a reverse period doubling cascade, as the coupling factor ξ is increased. So, depending on the value of ξ, the system can be in a chaotic or in a periodic state. The gap junction controls the flow of energy between the two neuron cells and suppresses the chaotic state of the system.

3.2. The system is driven by a DC voltage source

When the neuronal cells "ImK" and "RaLa" are uncoupled and stimulated by a low value DC signal, they create an action potential waveform, which converges to a fixed point, as we can see in Figs.8 and 9. As the value of the DC signal is increased, a Hopf bifurcation is observed and the neuronal cells give a periodic response. For the "ImK–cell" the Hopf bifurcation is observed for $U_{DC} = 0.29287$, while for the "RaLa–cell" the Hopf bifurcation is observed for $B_{DC} = 0.33233$, when the parameters of the system are a = 0.7, b = 0.8, c = 0.1 and ε = 0.150.

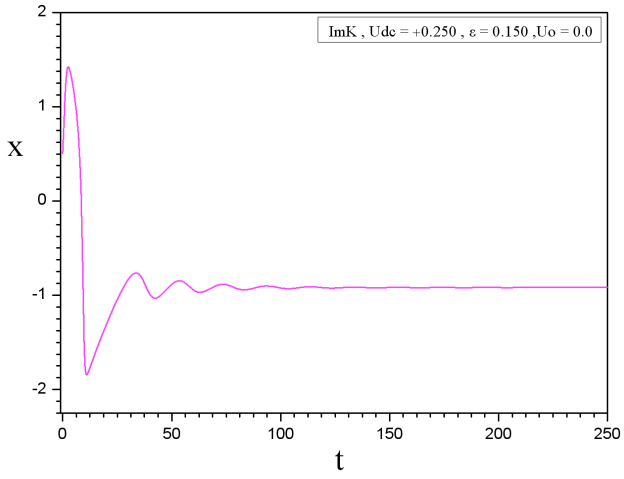

Fig. 8. Action potential waveform by an "ImK–cell" for $U_{DC} = 0.250$.

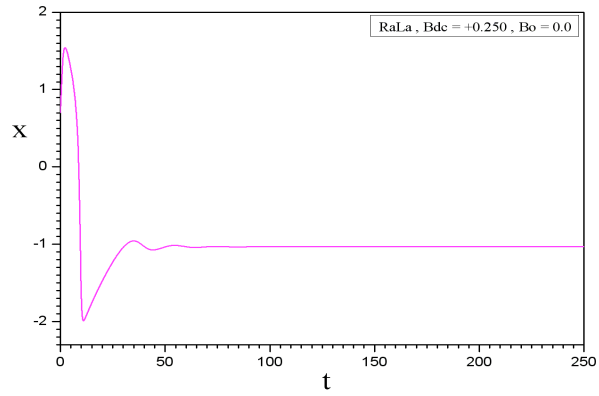

Fig. 9. Action potential waveform by a "RaLa–cell" for $B_{DC} = 0.250$.

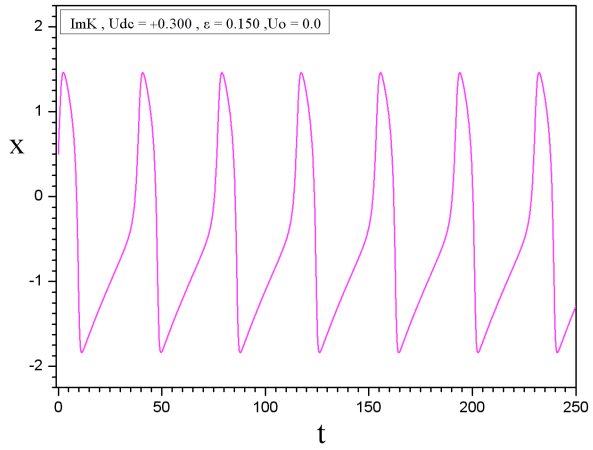

Fig. 10. A periodic response of an "ImK–cell" for $U_{DC} = 0.300$.

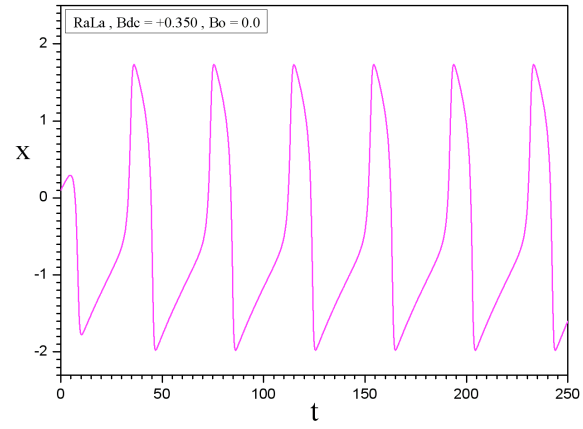

Fig. 11. A periodic response of a "RaLa–cell" for $B_{DC} = 0.350$.

In Figs.12 and 13, the bifurcation diagrams of the "ImK–cell" before, ($U_{DC} = 0.200$), and after, ($U_{DC} = 0.300$), the Hopf bifurcation threshold, are shown. We can clearly observe, that the two bifurcation diagrams are quite different for low values of U_0, but both follow a reverse period doubling route for high values of U_0.

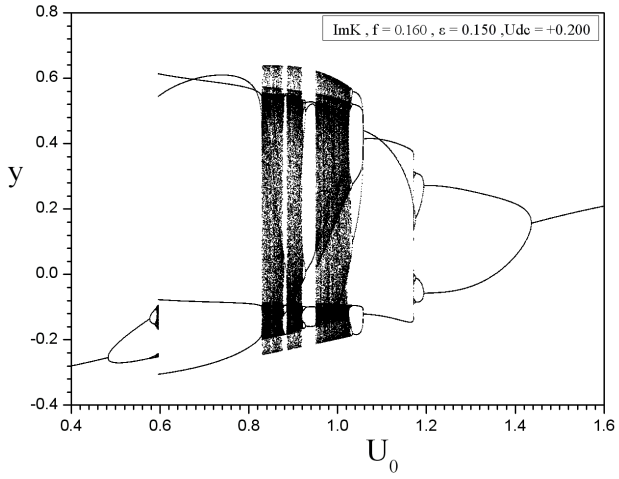

Fig. 12. The bifurcation diagram of the "ImK–cell" before, (U_{DC} = 0.200), the Hopf bifurcation threshold.

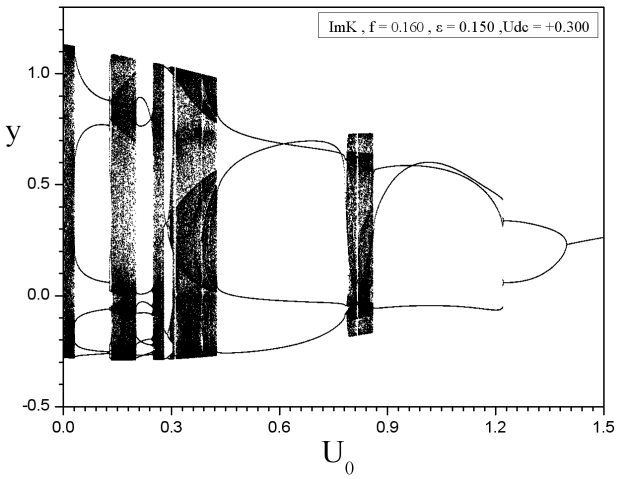

Fig. 13. The bifurcation diagram of the "ImK–cell" after, (U_{DC} = 0.300), the Hopf bifurcation threshold.

In the case of the coupled system of Fig.4, for U_{DC} = 0.250 and ξ = 0.01, the waveforms of the state variables x_1, (black), and x_2, (red), are shown in Fig.14. Both, they converge to a fixed point, as well as when U_{DC} = 0.300, (Fig.15).

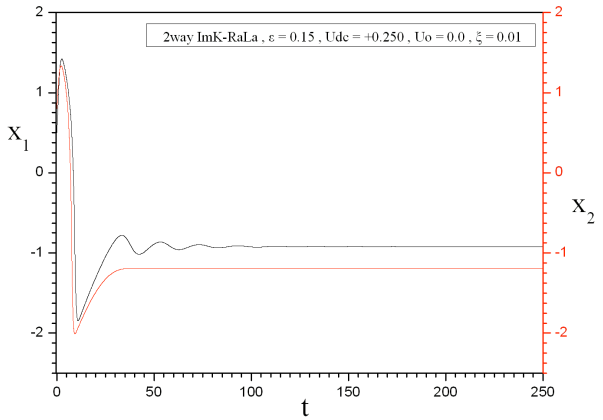

Fig. 14. The waveforms of the state variables x_1, (black), and x_2, (red), for U_{DC} = 0.250 and ξ = 0.01. Both, they converge to a fixed point.

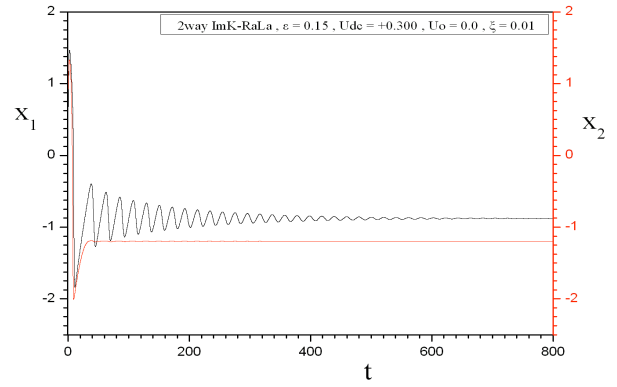

Fig. 15. The waveforms of the state variables x_1, (black), and x_2, (red), for U_{DC} = 0.300 and ξ = 0.01. Both, they converge to a fixed point.

In Figs.16 and 17, the responses of the coupled cells are shown, for U_{DC} = 0.350 and ξ = 0.01. They are periodic.

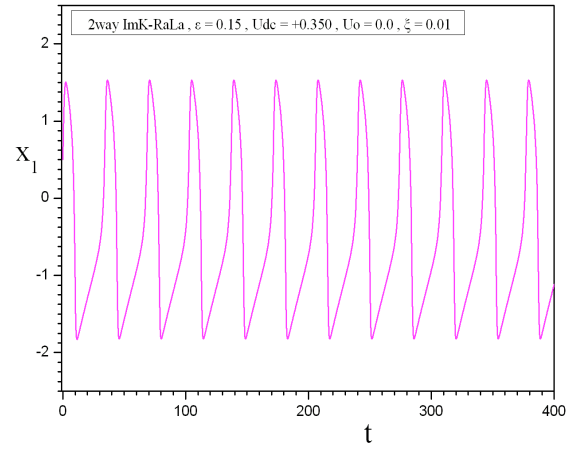

Fig. 16. Periodic response of the "ImK–cell" for U_{DC} = 0.350 and ξ = 0.01.

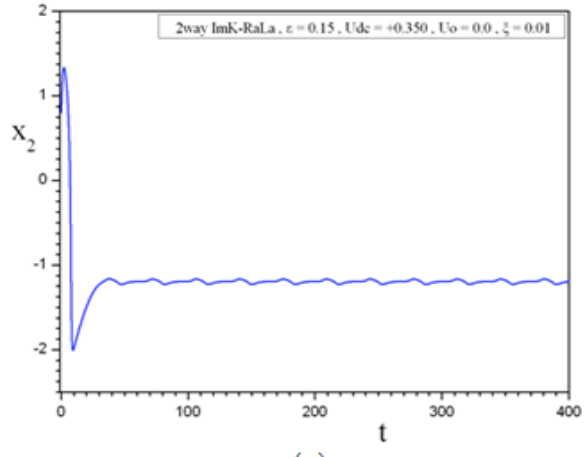

(a)

(continued)

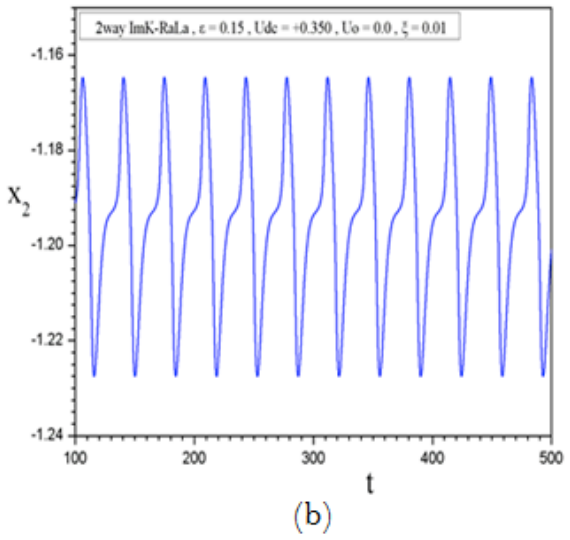

Fig. 17. The response of the coupled "RaLa–cell" for $U_{DC} = 0.350$ and $\xi = 0.01$. (a) Transients are present. (b) Transients have been removed, and a periodic response is shown, the steady state of the cell.

The dynamics of the system remains unchanged, as the value of the DC component is increased up to $U_{DC} = 1.00$. So, the next step is to increase the value of the coupling factor ξ. For $\xi = 0.074$, the phase portrait y_1 vs. x_1 is shown in Fig.18. It is a limit cycle. For $\xi = 0.075$, a period doubling is observed (Fig.19).

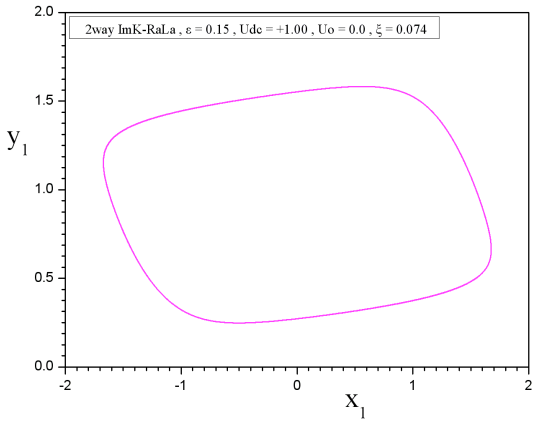

Fig. 18. Phase portrait of the coupled "ImK–cell" for $U_{DC} = +1.00$ and $\xi = 0.074$.

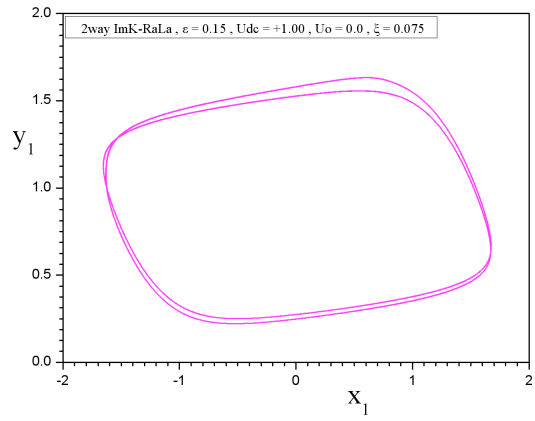

Fig. 19. Phase portrait of the coupled "ImK–cell" for $U_{DC} = +1.00$ and $\xi = 0.075$. A period doubling is observed.

As ξ is increased, the system follows a period adding scenario, as we can observe in Figs.20-22. For $\xi = 0.12739$, the phase portrait of the coupled "Rala-cell", for $U_{DC} = +1.00$, is shown in Fig.23. It is an attractor of high periodicity. In the limit, as periodicity tends to "infinity", a transition to period-1 is observed for $\xi = 0.12740$ (Fig.24).

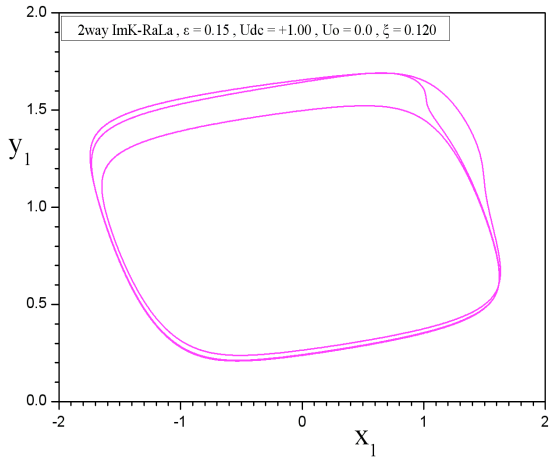

Fig. 20. Phase portrait of the coupled "ImK–cell" for $U_{DC} = +1.00$ and $\xi = 0.120$. A period–3 limit cycle is observed.

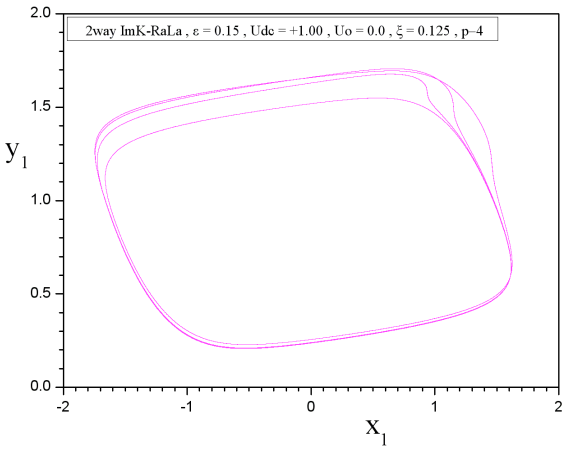

Fig. 21. Phase portrait of the coupled "ImK–cell" for $U_{DC} = +1.00$ and $\xi = 0.125$. A period–4 limit cycle is observed.

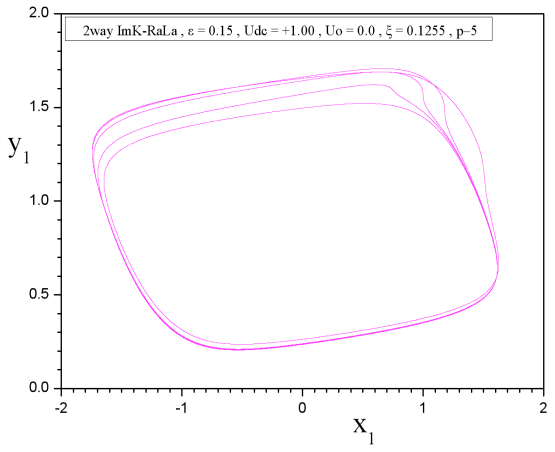

Fig. 22. Phase portrait of the coupled "ImK–cell" for $U_{DC} = +1.00$ and $\xi = 0.1255$. A period–5 limit cycle is observed.

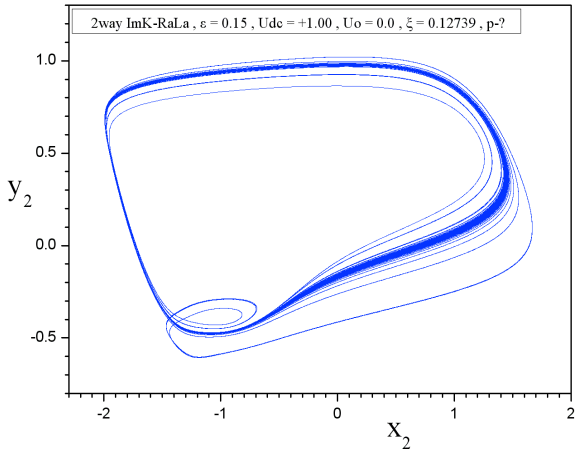

Fig. 23. The phase portrait of the coupled "Rala–cell", for $U_{DC} = +1.00$, and $\xi = 0.12739$. High periodicity.

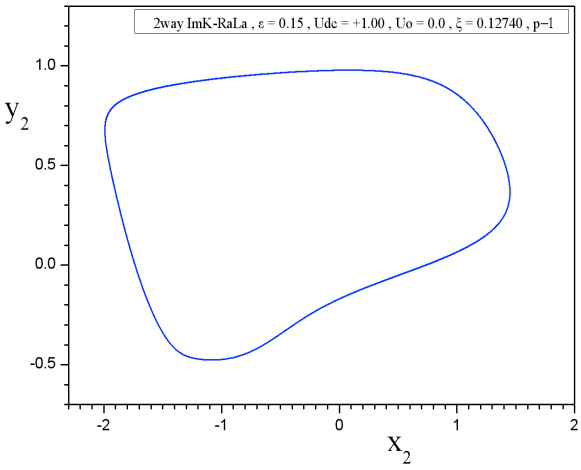

Fig. 24. The phase portrait of the coupled "Rala–cell", for $U_{DC} = +1.00$, and $\xi = 0.12740$. Period–1.

The bifurcation diagram, y_1 vs. ξ, for $U_{DC} = +1.00$, is shown in Fig.25, while the diagram of periodicity vs. ξ is shown in Fig.26, for up period–10. A staircase is formating, without chaos or quasiperiodicity between two nearby stairs.

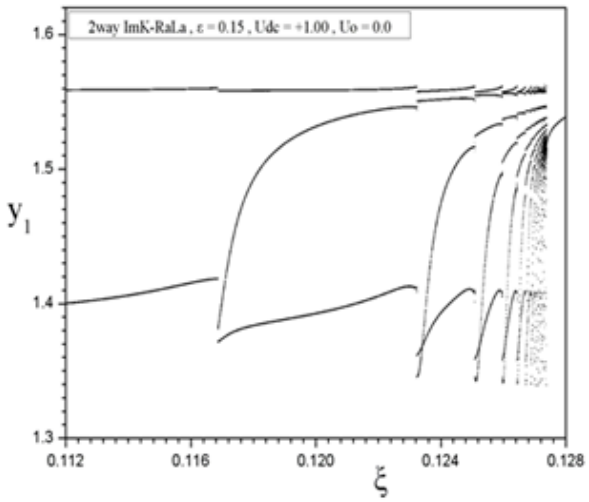

Fig. 25. Bifurcation diagram, y_1 vs. ξ, for $U_{DC} = +1.00$.

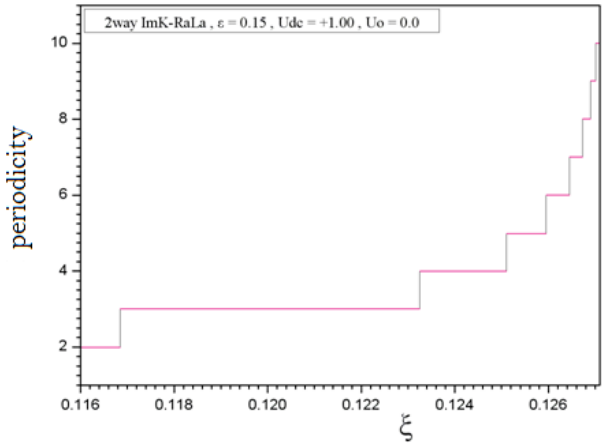

Fig. 26. Periodicity vs. ξ for $U_{DC} = +1.00$. A staircase is observed.

3.3. The system is driven by a DC plus an AC source

In the case of the combined stimulation of the system by a DC plus an AC voltage source, the dynamics show a more complex behavior, because each component, DC and AC, results to different dynamics, as the coupling factor ξ is varied. We will present some results, which show the necessity of an extended study.

3.3.1. The case $U_{DC} = +0.300$

For $U_{DC} = +0.300$, $U_0 = 0.0$ and $\xi = 0.01$, the system converges to a fixed point (Fig.15). If $U_0 \neq 0.0$ the dynamics are quite different. For $U_0 = 0.35$, and f = 0.16, the bifurcation diagrams versus the coupling factor are shown in Figs.27 and 28. We can observe the chaotic behavior of the system, while $\xi < 0.014$. For $\xi > 0.014$, the system converges to a period–1 limit cycle.

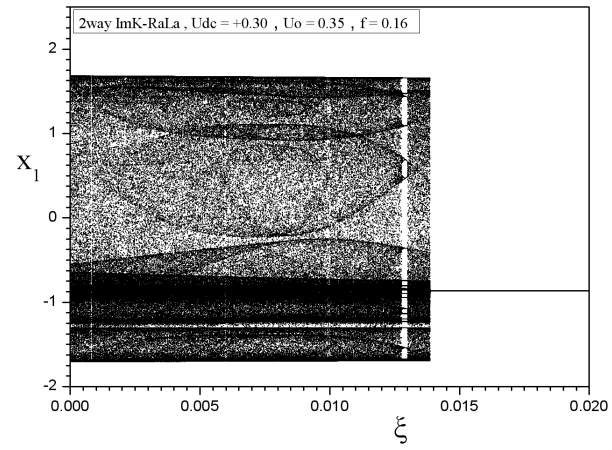

Fig. 27. Bifurcation diagram, x_1 vs. ξ, for $U_{DC} = +0.300$, $U_0 = 0.35$ and $f = 0.16$.

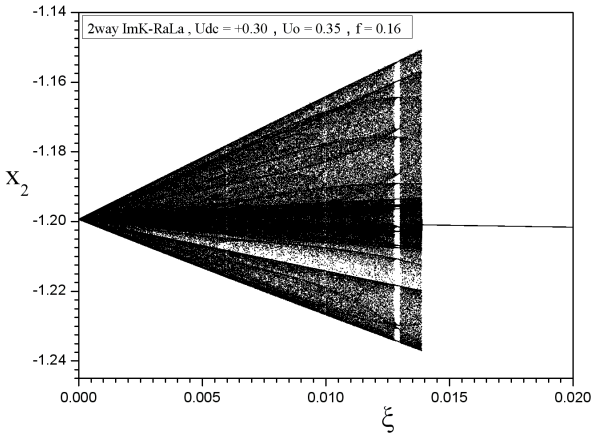

Fig. 28. Bifurcation diagram, x_2 vs. ξ, for $U_{DC} = +0.300$, $U_0 = 0.35$ and $f = 0.16$.

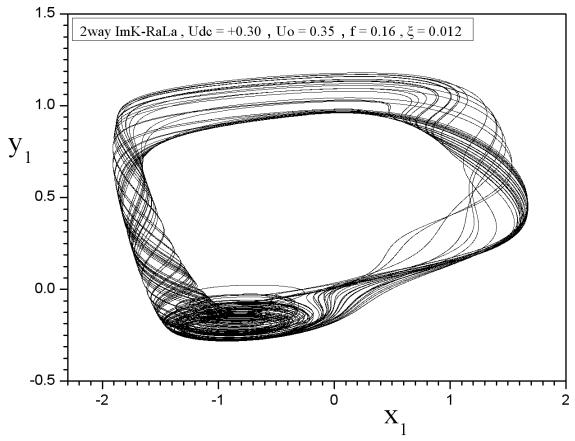

Fig. 29. Phase portrait, y_1 vs. x_1, of the "ImK–cell", for $U_{DC} = +0.300$, $U_0 = 0.35$, $f = 0.16$ and $\xi = 0.012$.

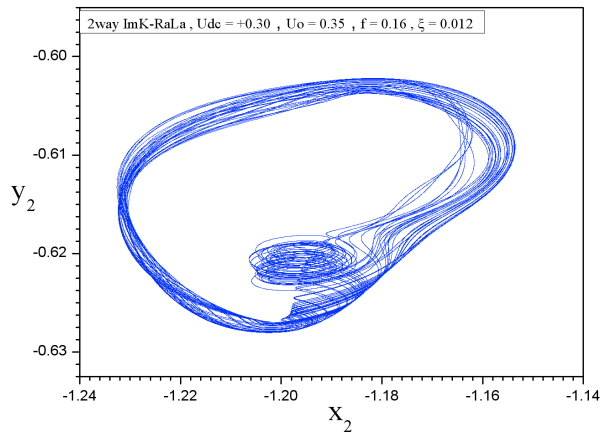

Fig. 30. Phase portrait, y_2 vs. x_2, of the "RaLa–cell", for $U_{DC} = +0.300$, $U_0 = 0.35$, $f = 0.16$ and $\xi = 0.012$.

For $U_0 = 0.4$, the system presents the same dynamics, as before, while the transition from chaos to period–1 is observed for a higher value of the coupling factor, $\xi = 0.0161$, as it is shown in Figs.31 and 32.

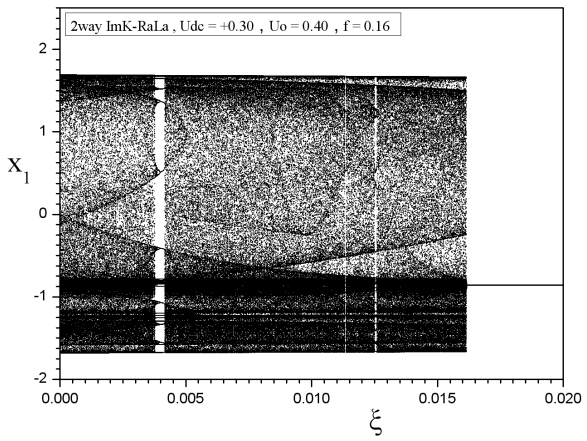

Fig. 31. Bifurcation diagram, x_1 vs. ξ, for $U_{DC} = +0.300$, $U_0 = 0.4$ and $f = 0.16$.

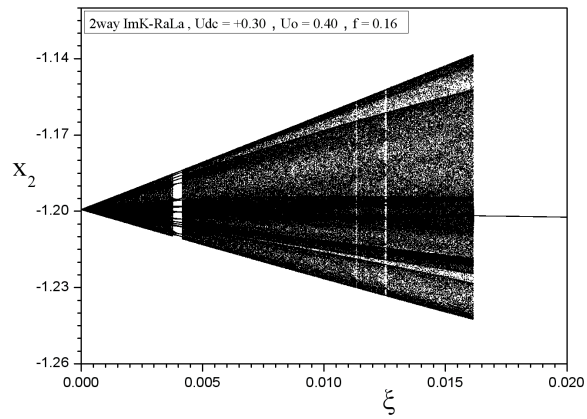

Fig. 32. Bifurcation diagram, x_2 vs. ξ, for $U_{DC} = +0.300$, $U_0 = 0.4$ and $f = 0.16$.

For $U_0 = 0.5$, the system remains in a periodic state for all values of the coupling factor. Starting from period–4, we observe a transition to period–1, for $\xi = 0.099$ (Figs.33 and 34).

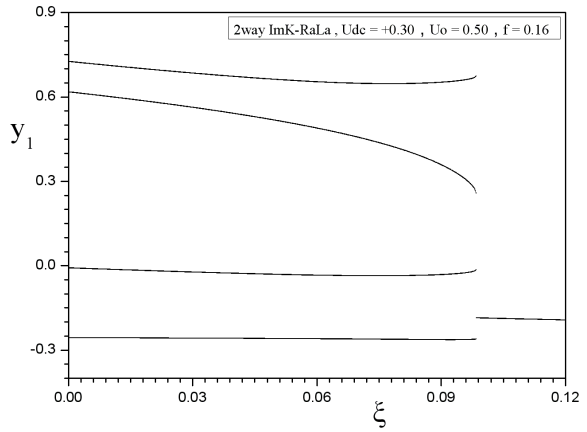

Fig. 33. Bifurcation diagram, y_1 vs. ξ, for $U_{DC} = +0.300$, $U_0 = 0.5$ and $f = 0.16$.

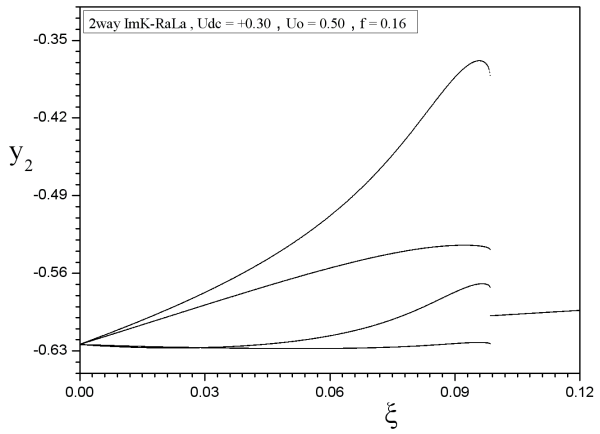

Fig. 34. Bifurcation diagram, y_2 vs. ξ, for $U_{DC} = +0.300$, $U_0 = 0.5$ and $f = 0.16$.

For $U_0 = 0.7$, chaotic behavior is also observed in a short regime, and, as the coupling factor is increased, the system follows a reverse period doubling up to period–1 (Figs.35 and 36). It is important to notice, that the two coupled cells have the same dynamics for any value of ξ.

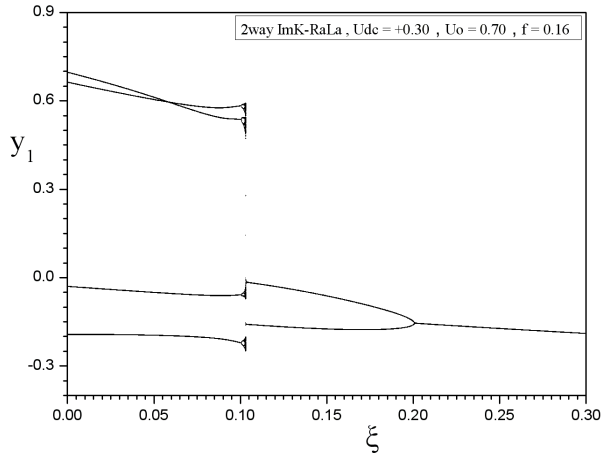

Fig. 35. Bifurcation diagram, y_1 vs. ξ, for $U_{DC} = +0.300$, $U_0 = 0.7$ and $f = 0.16$.

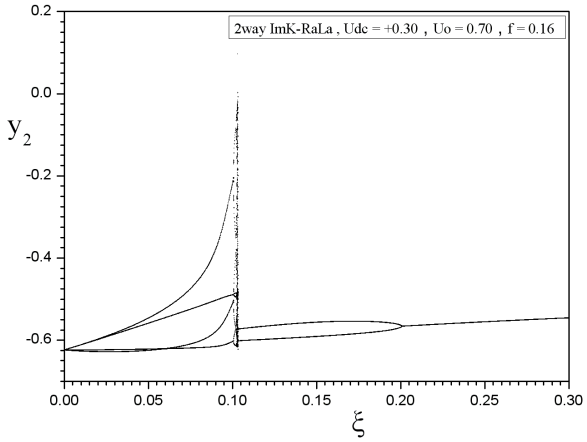

Fig. 36. Bifurcation diagram, y_2 vs. ξ, for $U_{DC} = +0.300$, $U_0 = 0.7$ and $f = 0.16$.

For $U_0 = 0.75$ the system starts from a periodic of period–4 state, then a chaotic regime is observed, more extended than in the case of $U_0 = 0.70$, and, as ξ is increased, a reverse period doubling is observed, up to period–1 (Figs.37 and 38).

For $U_0 = 0.8$ and $U_0 = 0.9$, chaotic regimes are also present, and as ξ is increased a reverse period doubling is observed, up to period–1 (Figs.39 and 40).

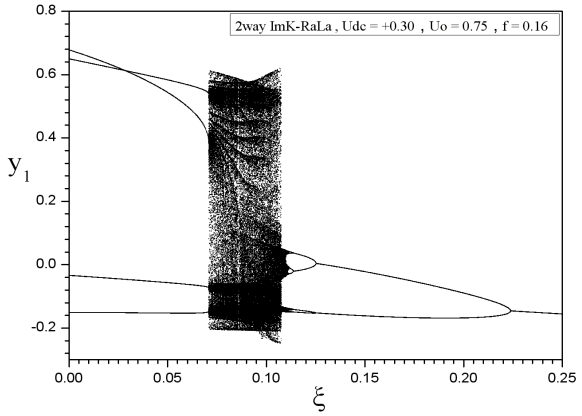

Fig. 37. Bifurcation diagram, y_1 vs. ξ, for $U_{DC} = +0.300$, $U_0 = 0.75$ and $f = 0.16$.

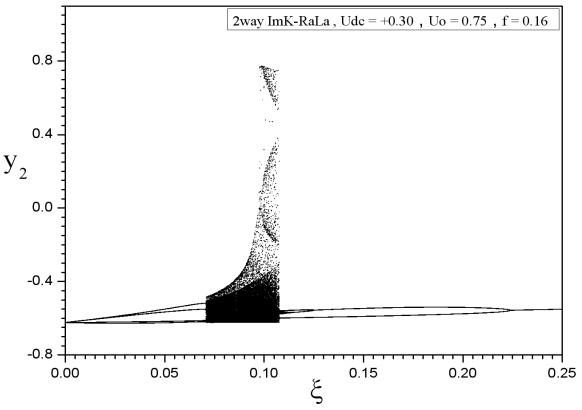

Fig. 38. Bifurcation diagram, y_2 vs. ξ, for $U_{DC} = +0.300$, $U_0 = 0.75$ and $f = 0.16$.

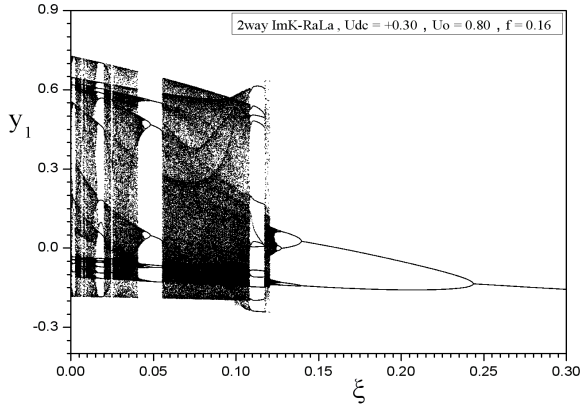

Fig. 39. Bifurcation diagram, y_1 vs. ξ, for $U_{DC} = +0.300$, $U_0 = 0.8$ and $f = 0.16$.

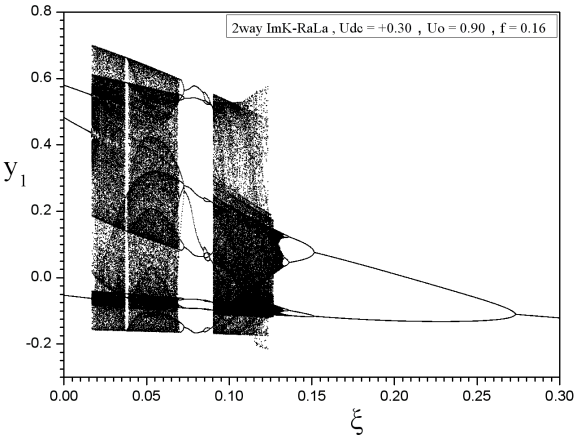

Fig.40. Bifurcation diagram, y_1 vs. ξ, for U_{DC} = +0.300, U_0 = 0.9 and f = 0.16 .

3.3.2. The case U_{DC} = +1.00

As the value of the DC component of the input signal is increased, more extended chaotic regimes are observed. In the case of U_{DC} = +1.00, for low values of the amplitude of the AC component of the input signal, the system remains, mainly, in chaotic state, even for high values of ξ, as we can observe in the bifurcation diagrams of Figures 41–43.

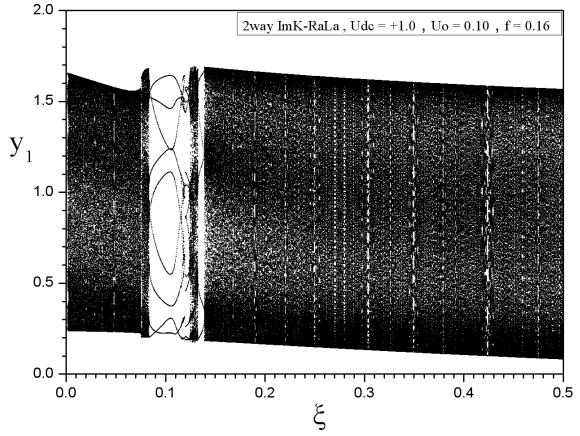

Fig. 41. Bifurcation diagram, y_1 vs. ξ, for U_{DC} = +1.00, U_0 = 0.1 and f = 0.16 .

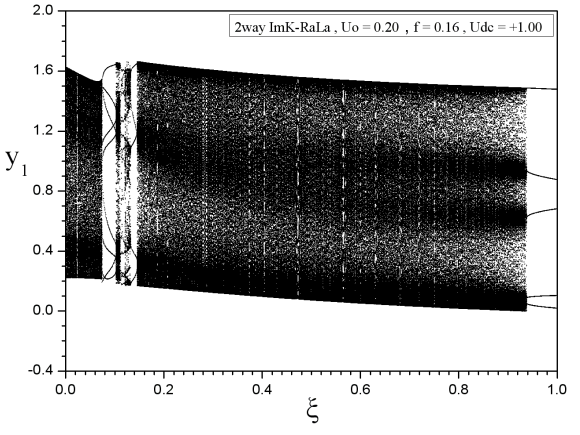

Fig. 42. Bifurcation diagram, y_1 vs. ξ, for U_{DC} = +1.00, U_0 = 0.2 and f = 0.16 .

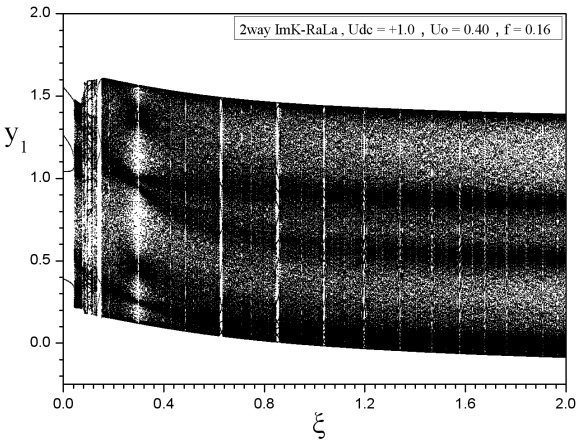

Fig. 43. Bifurcation diagram, y_1 vs. ξ, for U_{DC} = +1.00, U_0 = 0.4 and f = 0.16 .

The first wide periodic windows are observed for U_0 = 0.5, but they are of high periodicity (p–9, p–15), as it is shown in Fig.44.

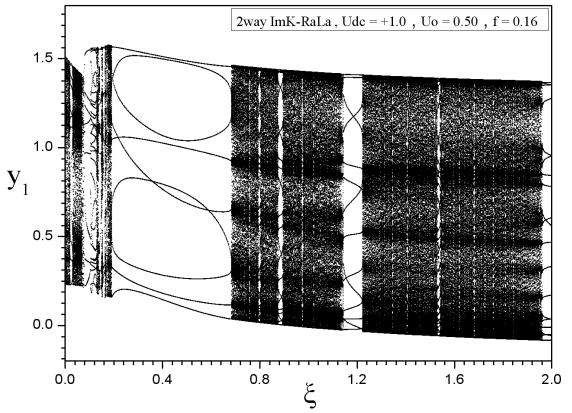

Fig. 44. Bifurcation diagram, y_1 vs. ξ, for U_{DC} = +1.00, U_0 = 0.5 and f = 0.16 .

As the amplitude U_0 is increased, the number of periodic windows are also increased (Figs.45, 46), so the system can choose its final state, periodic or chaotic. But its periodic state will be of high periodicity, no period–1.

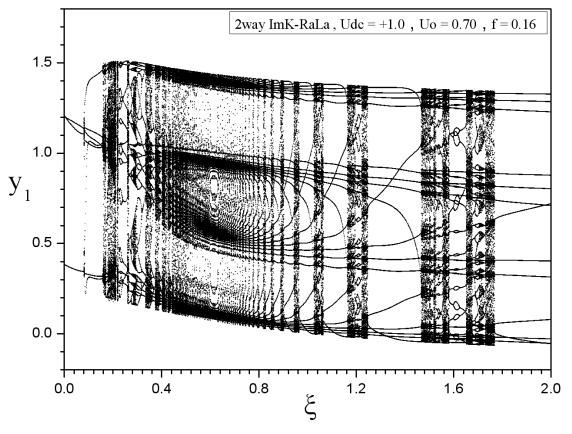

Fig. 45. Bifurcation diagram, y_1 vs. ξ, for U_{DC} = +1.00, U_0 = 0.7 and f = 0.16 .

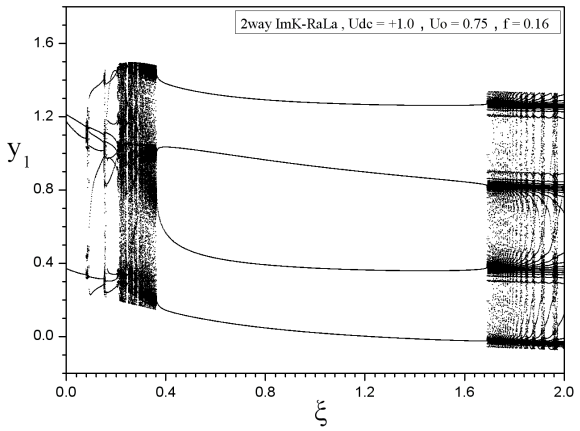

Fig. 46. Bifurcation diagram, y_1 vs. ξ, for $U_{DC} = +1.00$, $U_0 = 0.75$ and $f = 0.16$.

4. Conclusions

In the present paper, we have studied the complex dynamics of a system of two nonlinear neuronal cells, coupled by a gap junction, which is modelled as a linear variable resistor. The two coupled cells are oscillators of the FitzHugh–Nagumo type. The first cell, the "ImK–cell" is a voltage driven cell, while the second, the "RaLa–cell" is a current driven cell. We have examined the dynamics of the coupled system in the case of bidirectional coupling. An independent voltage source gives the external stimulation. When the external signal is an AC one, the system starting from a chaotic state undergoes a reverse period doubling and is driven to a period–1 steady state. In the case of a DC external signal, for low values of the signal, each cell, and also the whole system converge to a stable fixed point. As the DC signal is increased, a Hopf bifurcation occurs, and a periodic oscillation is observed. For higher values of the DC signal, $U_{DC} = +1.00$, as the coupling factor is increased the system follows a period adding route up to a certain value of the coupling factor, $\xi = 0.12740$, where a transition from "infinite" periodicity to a period–1 state is observed. The combined stimulation by a DC plus an AC voltage signals drives the system to chaotic states mainly. For low values of the DC signal, $U_{DC} = +0.30$, and $U_0 \geq 0.70$, a reverse period doubling sequence is observed, as the coupling factor is increased. For $U_{DC} = +1.00$, chaotic behavior is the main dynamics of the system. Some periodic windows in the bifurcation diagrams are observed for higher values of the amplitude of the AC external signal.

References

1. R. FitzHugh, Biophys. J. **1**, 445 (1961).
2. J. Nagumo, S. Arimoto, and S. Yoshizawa, Proc. IRE **50**, 2061 (1962).
3. W. Jiang, D. Bin, and K. M. Tsang, Chaos Solitons & Fractals **22**, 469 (2004).
4. M. Aqil, K-S. Hong, and M-Y. Jeong, Commun. Nonlinear Sci. Numer. Simlat. **17**, 1615 (2012).
5. A. L. Hodgkin and A. F. Huxley, J. Physiol. **117**, 500 (1952).
6. I. M. Kyprianidis, V. Papachristou, I. N. Stouboulos and Ch. K. Volos, WSEAS Trans. Syst. **11**, 516 (2012).
7. S. Rajasekar and M. Lakshmanan, Physica D **32**, 146 (1988).
8. S. Rajasekar and M. Lakshmanan, Physica D **67**, 282 (1993).